

# A Novel Genetic Algorithm with db4 Lifting for Optimal Sensor Node Placements

Ganesan Thangavel\*

Department of Computer Science and Engineering,  
Koneru Lakshmaiah Education Foundation, India  
tganesanit@gmail.com

Pothuraju Rajarajeswari

Department of Computer Science and Engineering,  
Koneru Lakshmaiah Education Foundation, India  
rajilikhitha@gmail.com

**Abstract:** Target coverage algorithms have considerable attention for monitoring the target point by dividing sensor nodes into cover groups, with each sensor cover group containing the target points. When the number of sensors is restricted, optimal sensor node placement becomes a key task. By placing sensors in the ideal position, the quality of maximum target coverage and node connectivity can be increased. In this paper, a novel genetic algorithm based on the 2-D discrete Daubechies 4 (db4) lifting wavelet transform is proposed for determining the optimal sensor position. Initially, the genetic algorithm identifies the population-based sensor location and 2-D discrete db4 lifting adjusts the sensor location into an optimal position where each sensor can cover a maximum number of targets that are connected to another sensor. To demonstrate that the suggested model outperforms the existing method, A series of experiments are carried out using various situations to achieve maximum target point coverage, node interconnectivity, and network lifetime with a limited number of sensor nodes.

**Keywords:** Wireless sensor network, target point coverage, node connectivity, sensor deployment, genetic algorithm, two-dimensional db4 lifting, network lifetime.

Received March 19, 2021; accepted October 21, 2021  
<https://doi.org/10.34028/iajit/19/5/12>

## 1. Introduction

In recent years, wireless sensor node deployment has resulted in a vast variety of sensor nodes that are being researched due to their potential sensing, wireless communication, and data processing capabilities [6]. The sensor nodes in the various surveillance applications are geographically scattered [23]. Due to insufficient energy sources, a sensor can only be operational for a certain amount of time.

Sensor deployment and target coverage are other key critical issues in WSNs, which affect the sensor network lifetime [27]. The sensors can be deployed in two techniques known as random and deterministic sensor deployment. When the sensing field was very large and in a remote, hostile, and inaccessible place, random sensor deployment was used [18, 25]. In this critical case, sensors might be deployed randomly to be the best choice. The sensors are scattered randomly in the sky over the aircraft or new approach, resulting in falling at any location in the field.

Deterministic sensor deployment is used to select the optimum position for attaining network design objectives such as network coverage, network cost, network lifetime, and connection with a limited number of sensor nodes. The coverage types can be categorized into the area [13], barrier, and target coverage. Thus, sensors are coordinated into different sensor cover groups, whereas each sensor monitors the set of target points for a specific duration when the optimal use of

sensors increases the network lifetime [24]. Also, sensors are organized into different connectivity groups which can be able to communicate with any sensor in the optimal location [21]. Optimized node deployment over the target point coverage and node connectivity draws a lot of attention in the WSNs research community [11].

The main objective of the paper is as follows, a novel Genetic Algorithm (GA) with 2-D Discrete Daubechies 4 Lifting Wavelet Transform (2D D db4 LWT) is introduced for optimal sensor placement in target point coverage and node connectivity problem. Initially, random sensor coordinate populations matrices are generated based on a genetic algorithm and it is applied into a fitness function to evaluate the quality of maximum target coverage. Further, population matrices are applied into crossover, and mutation operation to improve the sensor coordinate position. Finally, discrete Daubechies 4 lifting wavelet transform based local enhancement to improve the quality of maximum target coverage and node connectivity and minimized energy consumption as to be optimum. The rest of the sections consist of related works as shown in section 2. Section 3 described the problem formulation of the proposed methodology. Section 4 explains about discrete Daubechies lifting wavelet transform for the level-by-level matrix decomposition model. Section 5 deals with the implementation of the proposed novel GA and 2D D db4 LWT with a suitable number of sensor nodes and target points. Section 6 validates the performance of

proposed methods in terms of target cover sets, sensor connect sets, and sensor energy models with different scenarios. Section 7 provides the conclusion and future enhancement followed by a reference section.

## 2. Related Work

To extend the network lifetime, and optimal coverage of mobile Wireless Sensor Networks (MWSN), Abo-Zahhad *et al.* [2] developed a Centralized Immune-Voronoi Deployment Algorithm (CIVA) to maximize the coverage by using binary and probabilistic models. The Vilela *et al.* [33] presented the static sensor for dynamic networks by Iso-Probability curves based on mobile target coverage.

The Moh'd Alia and Al-Ajouri [26] stated that the probability of coverage ratio is categorized into fully covered, partially (un)covered, and uncovered patterns. A novel stochastic physics-based optimization algorithm was proposed by Njoya *et al.* [28], the authors addressed the full target coverage, whereas the move, merge, recombine, and explode process was performed by virtual sensors. The Nguyen *et al.* [27] formulated the Integer Linear Programming (ILP) method for target coverage. The ILP method computes target coverage with a smaller number of sensor nodes [24].

The network lifetime depends on the number of Disjoint Sets Covers (DSC) groups. The Ashouri *et al.* [3] focused on the DSC and k-coverage problem by using the Boolean Satisfiability (SAT) method. Chen *et al.* [6] also utilized DSC with Dynamic Coverage Maintenance (DCM) to maximize the network lifetime when a hybrid memetic framework was applied to the random populations. Along with k-coverage, the Mini *et al.* [25] further extended this work with a 1-coverage to improve the network lifetime and Q-coverage to cover every target by q-sensor nodes. Gupat *et al.* [12] have examined the k-coverage to each target and m-connectivity to all sensor nodes based on a GA. The method [7, 9, 10] achieved continuous monitoring of certain targets for a long time with minimum energy, whereas an optimum number of cover head selection was based on GA. Liao and Ting [23] applied a novel integer-coded Memetic Algorithm (MA) for the set k-cover and tighter upper bound to reduce the search space.

The random position of sensor coordinates was adjusted by Two-Dimensional Discrete Haar Wavelet Transform (2DDHWT) for local enhancement after the memetic algorithm based on random deployment of population matrix by Vijayaraju *et al.* [32]. The point-coverage and area coverage disjoint set cover problems were represented by forwarding encoding scheme-based schedule transition hybrid GA [19, 25]. Area coverage Yoon and Kim *et al.* [34] has also been solved by GA-based random deployment, in addition to the phenotype space problem. This problem is a quotient space of genotype space and computation time is reduced by the

Monte Carlo method.

The Next-Generation Networks (NGN) problems were explained by Abdelkhalik *et al.* [1], whereas decision supported system is applied in a multi-objective Variable-Length Genetic Algorithm (VLGA) based on heterogeneous networks. In addition to VLGA, Zhang *et al.* [36] addressed the Flexible Genetic Algorithm (FGA) with swap-area crossover, Gaussian mutation to the wind farm, and Radio Frequency Identification (RFID) placements. Thi Hanh *et al.* [13] combined GA with Laplace X-point crossover (LX) and Arithmetic X-Point Crossover Operation (AMXO) to produce two different offspring for the Virtual Force Algorithm (VFA) based on the local search method. Katii [21] modeled the homogeneous networks for target coverage duration, more target cover sets, and minimum energy path node connectivity with maximum network lifetime [17].

The Bouzid *et al.* [5] have presented the Multi-Objective Optimization of A Wireless Network Using A Genetic Algorithm (MOONGA) for sensing coverage based on the degree of sensing coverage k, connectivity was assessed based on the degree of connectivity m to avoid redundancy of sensing coverage. Zhang *et al.* [35] have extended the multi objectives optimization to degressive Ary number encoded GA for node placements. The Karimi-Bidhendi *et al.* [20] had discussed Heterogeneous Two-Tier- Lloyd (HTTL) algorithm to minimize the two-tier power consumption for optimal node deployment. The Fan *et al.* [8] focused on homogeneous WSN and non-uniform sensor deployment to analyze the node density using Probability Density Function (PDF) using the energy consumption model.

The Harizan and Kuila [14] presented NSGA-II with modified dominance for scheduling problems in node coverage, connectivity, and energy consumption. It has a minimum number of sensor nodes, full coverage with connectivity between the base stations, and to select the higher energy level for scheduling [16]. The Pal *et al.* [29] computed IEEE802.15.4 based real-time monitoring system for potato and wheat crops-based node connectivity. The Kim and Yoo [22] formulated the sensor target coverage problem using Bat Algorithm (BA) whereas, one bat finds the activated sensor node for sensing and others finds the data forwarding from the active sensor to a sink.

## 3. Problem Formulation

### 3.1. Network Model

Suppose a set of m targets are distributed as  $T = \{T_k : \forall k \in \{1 \leq k \leq m\}\}$  where the target  $T_k$  is deployed in a random location in the region  $A^*A$ . Also, a set of n sensors are distributed randomly, where  $S_i$  and  $S_j$  are the sensors in the same region  $A^*A$  to monitor the target  $T_k$ . To ensure network connectivity, each sensor

node must perceive the sensing range RS and have a communication range RC of at least 2RS. The main objective is to discover optimal positions of n sensors to cover or monitor the given m target points ( $S(n) \leq T(m)$ ) to achieve the maximum number of targets covers, node connectivity, and network lifetime.

### 3.2. Coverage Model

The target  $T_k$  is deployed randomly in the region shown in Figure 1.  $(X_k, Y_k)$  and sensors  $S_i$  and  $S_j$  are also located in the position  $(X_i, Y_i), (X_j, Y_j)$  in a similar region with  $RS_i, RS_j$  sensing range, respectively. To fulfill the distance between the sensor position and the target location, the sensors  $S_i$  or  $S_j$  are performed to monitor the target  $T_k$ . (1). Each target is served by at least one sensor node. If the target  $T_k$  is covered by  $S_i$  or  $S_j$ ,  $T_k$  is added to the CV cover set (2). Initially, all the sensors are having an empty cover set of targets  $\phi \subseteq S$ , and all the targets should be covered by at least one sensor node. A Coverage set CV is defined as  $C_v \subseteq S$ , if the sensor  $S_i$  monitors the target  $T_k$  then, it is added to the  $\{S_i\}$  cover set.

$$d(S_i, T_k) = \sqrt{(X_i - X_k)^2 + (Y_i - Y_k)^2} \tag{1}$$

$$C_{vi} = \{S_i\} = \begin{cases} 1, & d(S_i, T_k) \leq R_{Si} : \forall i \in \{1 \leq i \leq n\}, \forall k \in \{1 \leq k \leq m\} \\ 0, & \text{otherwise} \end{cases} \tag{2}$$

### 3.3. Connectivity Model

The  $C_n$  represents the set of sensor nodes within the RC communication range. The sensors  $S_i$  and  $S_j$  can communicate data if the Boolean condition is met (3).

The connectivity set  $C_n$  is defined as  $C_n \subseteq S$  when, the sensor  $S_i$  communicates to  $S_j$  then, it is added to the connectivity set (4). The connectivity Boolean condition is defined as

$$d(S_i, S_j)^2 = (X_i - X_j)^2 + (Y_i - Y_j)^2 \tag{3}$$

$$C_{ni} = \{S_i\} = \begin{cases} 1, & d(S_i, S_j) \leq 2R_C : \forall i, j \in \{1 \leq i, j \leq n\} \\ 0, & \text{otherwise} \end{cases} \tag{4}$$

### 3.4. Potential Position

The potential position of each sensor is identified as when the sensor can cover at least one target and can communicate with any one of the sensors. The potential position of each sensor  $PS_i$  and target covered can be represented mathematically using a potential matrix (5) and (6). The  $PS_i$  of every sensor along with target  $T_k$  can be represented in a Boolean matrix as given below.

$$PS_i = \begin{cases} 1, & C_{vi} \exists 1, C_{ni} \exists 1 : \forall i, j \in \{1 \leq i, j \leq n\} \\ 0, & \text{otherwise} \end{cases} \tag{5}$$

$$PS_{(n,m)} = \begin{bmatrix} PS_1 & T_1 & T_2 & \dots & T_k & T_m \\ PS_{1,1} & PS_{1,2} & \dots & PS_{1,k} & PS_{1,m} \\ PS_2 & PS_{2,1} & PS_{2,2} & \dots & PS_{2,k} & PS_{2,m} \\ \dots & \dots & \dots & \dots & \dots & \dots \\ PS_i & PS_{i,1} & PS_{i,2} & \dots & PS_{i,k} & PS_{i,m} \\ PS_n & PS_{n,1} & PS_{n,2} & \dots & PS_{n,k} & PS_{n,m} \end{bmatrix} \tag{6}$$

The above  $PS(n, m)$  matrix can be signified as a column-wise sum  $\tau_k$  to measure the quality of the potential position using (7) and (8).

$$\tau = (\tau_1, \tau_2, \dots, \tau_k, \dots, \tau_m), \text{ where} \tag{7}$$

$$\tau_k = \sum_{i=1}^m \sum_{j=1}^n (PS_{i,k}) \exists 1$$

$$QPS(\%) = \left( \frac{\sum_{k=1}^m \left( \frac{\tau_k}{n} \right)}{n} \right) \times 100 \tag{8}$$

### 3.5. Energy Model

The network lifetime is determined by the primary battery power  $b_i$  and energy consumption rate  $e_i$  of each sensor. The duration of battery power in terms of time is defined. The tight upper bound  $U$  (9) denotes the maximum network lifetime that can be achieved when each sensor covers at least one target.

$$b_i^p = \left( \frac{b_i}{e_i} \right) : \forall i \in \{1 \leq i \leq n\} \tag{9}$$

$$U = \left\{ \min_{k \in m} \left( \frac{\sum_{i=1}^n PS_{i,k} * b_i^p}{n} \right) \right\}$$

### 4. Lifting Wavelets

The Daubechies wavelet (db4) has two wavelet analysis processes as wavelet function ( $\psi(t)$ ) recognized as the mother wavelet (10) and the scaling function ( $\varphi(t)$ ) recognized as the father wavelet (11). This analysis function can be stated as follows,

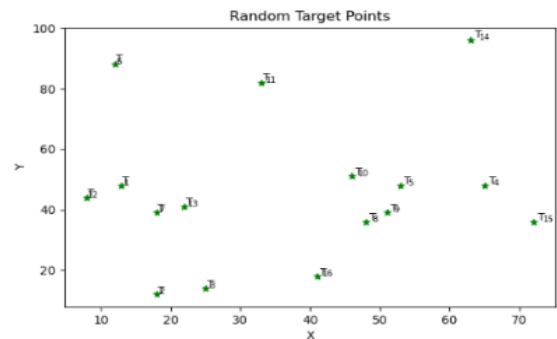


Figure 1. Random target points deployment.

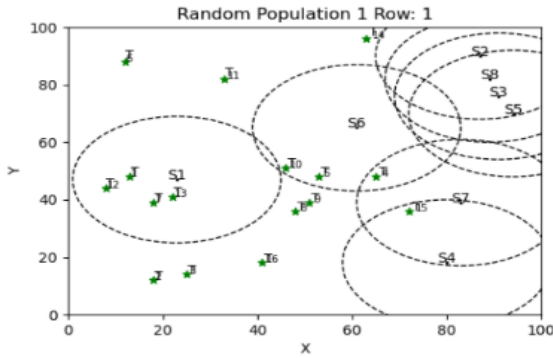


Figure 2. Random sensor pp 1 row 1 deployment.

$$\varphi(t) = f(z) = f_0 + f_1(z^{-1}) + f_2(z^{-2}) + f_3(z^{-3}) = \sum_{l=0}^{l=3} f_l(z^{-l}) \quad (10)$$

$$\psi(t) = g(z) = g_0 + g_1(z^{-1}) + g_2(z^{-2}) + g_3(z^{-3}) = \sum_{l=0}^{l=3} g_l(z^{-l}) \quad (11)$$

The db4 wavelet has four vanishing moments. Wavelet analysis function  $\psi(t)$  and  $\varphi(t)$  has four coefficients  $(g_0, g_1, g_2, g_3)$  and  $(f_0, f_1, f_2, f_3)$  respectively. The coefficients values are as follows,

$$f_0 = \frac{1+\sqrt{3}}{4\sqrt{2}} \quad f_1 = \frac{3+\sqrt{3}}{4\sqrt{2}} \quad f_2 = \frac{3-\sqrt{3}}{4\sqrt{2}} \quad f_3 = \frac{1-\sqrt{3}}{4\sqrt{2}}, \quad g_0 = f_3 \quad g_1 = -f_2 \quad g_2 = f_1 \quad g_3 = -f_0$$

The  $\psi(t)$  and  $\varphi(t)$  can be represented as poly-phase data and poly-phase matrixs (12), and (13).

$$f(z) = f_e(z^2) + z^{-1}f_o(z^2), \quad g(z) = g_e(z^2) + z^{-1}g_o(z^2) \quad (12)$$

$$\rho(z) = \begin{bmatrix} f_e(z) & f_o(z) \\ g_e(z) & g_o(z) \end{bmatrix} = \begin{bmatrix} f_0 + f_2(z^{-1}) & -f_1 - f_3(z^{-1}) \\ f_1 + f_3(z^{-1}) & -f_0 + f_2(z^{-1}) \end{bmatrix} \quad (13)$$

The above poly-phase matrix can be factorized to get  $\rho(z)$  and  $\rho(z)^{-1}$  are expressed as follows (14):

$$\rho(z)^{-1} = \begin{bmatrix} \frac{\sqrt{3}-1}{\sqrt{2}} & 0 \\ 0 & \frac{\sqrt{3}+1}{\sqrt{2}} \end{bmatrix} \begin{bmatrix} 1 & -z \\ 0 & 1 \end{bmatrix} \begin{bmatrix} -\left(\frac{\sqrt{3}}{4} + \frac{\sqrt{3}-2}{4}(z^{-1})\right) & 0 \\ 1 & 1 \end{bmatrix} \begin{bmatrix} 1 & \sqrt{3} \\ 0 & 1 \end{bmatrix} \quad (14)$$

Based on the poly-phase matrix with even and odd sample approximate  $\lambda$  and detailed  $\delta$  coefficient using db4 forward lifting wavelet transform can be derived.

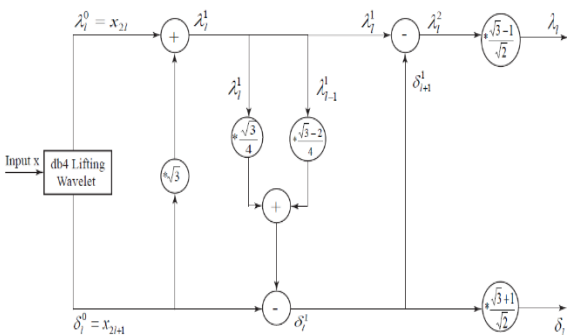


Figure 3. Block diagram of db4 lifting wavelet transform.

The input signal  $x(n)$  can be split into even  $x_{2l}$  and odd  $x_{2l+1}$  samples. The even sample is updated through the odd sample, whereas the odd sample is predicted

through the even samples. Finally, normalization is to be applied for all even and odd samples [30, 31]. These steps can be represented as shown in Figure 3. and expressed mathematically in (15) to (19).

$$Split(S) : \lambda_l^0 = x_{2l} \text{ (even)}, \delta_l^0 = x_{2l+1} \text{ (odd)} \quad (15)$$

$$Update1(U1) : \lambda_l^1 = \lambda_l^0 + \sqrt{3}\delta_l^0 \quad (16)$$

$$Predict(P) : \delta_l^1 = \delta_l^0 - \frac{\sqrt{3}}{4}\lambda_l^1 - \frac{\sqrt{3}-2}{4}\lambda_{l-1}^1 \quad (17)$$

$$Update2(U2) : \lambda_l^2 = \lambda_l^1 - \delta_{l+1}^1 \quad (18)$$

$$Normalize(N) : \lambda_l = \frac{\sqrt{3}-1}{\sqrt{2}}\lambda_l^2, \delta_l = \frac{\sqrt{3}+1}{\sqrt{2}}\delta_l^2 \quad (19)$$

In general, 2-D input data can be used to build the db4 lifting wavelet by first applying the 1-D row-wise db4 lifting wavelet transform and then the 1-D column-wise db4 lifting wavelet transform, as shown in Figure 4. This process will produce one approximate coefficient (LL) and three detailed sub-band (LH, HL, and HH).

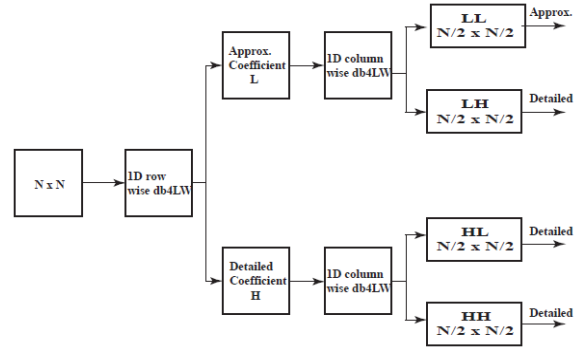


Figure 4. Conventional 2-D db4 lifting wavelet transform.

In Figure 5. The  $n \times n$  matrix can be reduced into  $\frac{n}{2} \times \frac{n}{2}$ , the approximate coefficient LL can be applied using level 2 db4 lifting to produce  $\frac{n}{4} \times \frac{n}{4}$  a submatrix. Here db4 lifting is used in the approximate submatrix Low Low (LL) in every level until it reaches the  $j$ th level as presented in Figure 5. The matrix  $n \times n$  is computed up to a  $j$ th level of the matrices [4, 15].

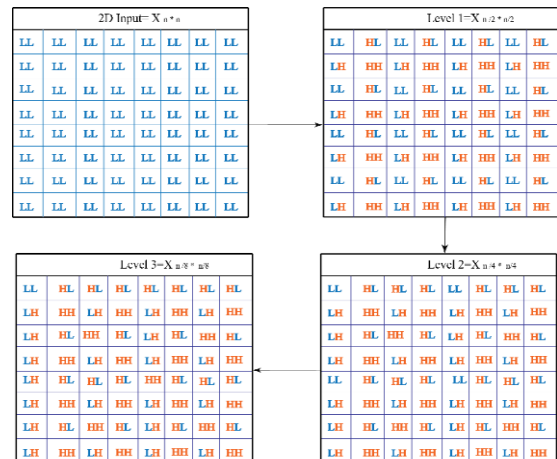


Figure 5. Decomposition of 2-D by db4 lifting wavelet transform.

### 5. nGA -2D db4 LW for Optimal Sensor Placement

GA's design was inspired by natural mechanisms like selection, crossover, and mutation. GA generates initial population matrices that contain the random location of each sensor. The fitness function is applied to each chromosome in the population matrix for a potential position. To improve the quality of the solution, the next generation will contribute gene exchange (crossover) and change gene values (mutation). In addition, in the local search, a 2D discrete db4 lifting wavelet transform is presented to change the prospective position of sensors. The final Quality Of Potential Position (QPS) is selected based on an optimized solution using survival operators from the parent population matrices and the child matrices to the next level. This process computes the maximum number of populations.

- **Initial Population:** random initialization is used to generate the initial population matrices as chromosomes ( $\Phi$ ). The scope of the population matrix is  $n \times n$ , where  $n$  is the total number of sensors. For individual chromosomes, the gene ( $\phi_{ij}$ ) generates a random number within the range 0 to  $A \times A$ , where  $A$  denotes the region size. Meanwhile, every row in a chromosome indicates the position of  $n$  sensors.

$$\Phi = \begin{bmatrix} s_1 & s_2 & \dots & s_i & s_n \\ \phi_{11} & \phi_{12} & \dots & \phi_{1i} & \phi_{1n} \\ \phi_{21} & \phi_{22} & \dots & \phi_{2i} & \phi_{2n} \\ \dots & \dots & \dots & \dots & \dots \\ \phi_{n1} & \phi_{n2} & \dots & \phi_{ni} & \phi_{nn} \end{bmatrix} \leftarrow \text{rand} \in (0, A * A)$$

To search the optimal position for every sensor, a set of 10 initial populations is generated randomly. The  $pp_1$  and  $pp_2$  are two randomly generated populations with size  $8 \times 8$ . The entry of each population chromosome gene is assigned to the random value from 0 to 10000.

$$pp_1 = \begin{bmatrix} 2347 & 8790 & 9176 & 8018 & 9470 & 6165 & 8339 & 8982 \\ 3772 & 9335 & 1484 & 1597 & 1783 & 4730 & 8179 & 3892 \\ 5685 & 5368 & 7875 & 9527 & 5235 & 3599 & 4013 & 3037 \\ 8870 & 5971 & 6474 & 9123 & 8197 & 6352 & 6427 & 4915 \\ 3381 & 3462 & 3990 & 5929 & 2438 & 3465 & 2059 & 2320 \\ 5903 & 1375 & 2245 & 9381 & 5104 & 4471 & 6319 & 6286 \\ 7275 & 4799 & 1355 & 2963 & 2684 & 2497 & 1509 & 3387 \\ 4638 & 3516 & 8850 & 6169 & 4227 & 7161 & 2471 & 9633 \\ 2953 & 2477 & 2240 & 1136 & 1745 & 1418 & 2482 & 9352 \\ 1323 & 2598 & 3270 & 2126 & 5699 & 4806 & 5428 & 8261 \\ 6672 & 3397 & 2715 & 8424 & 2132 & 7514 & 3122 & 5505 \\ 3101 & 6473 & 9497 & 9110 & 3248 & 9375 & 2459 & 3859 \\ 2383 & 9044 & 4122 & 2911 & 7737 & 5314 & 2918 & 3245 \\ 9479 & 8909 & 5374 & 2118 & 5837 & 3420 & 7277 & 2670 \\ 1652 & 4648 & 9755 & 1278 & 6236 & 6710 & 9561 & 8092 \\ 9982 & 2058 & 6265 & 8686 & 5055 & 2857 & 2461 & 7385 \end{bmatrix} \leftarrow \text{rand} \in (0,10000)$$

$$pp_2 = \begin{bmatrix} 2347 & 8790 & 9176 & 8018 & 9470 & 6165 & 8339 & 8982 \\ 3772 & 9335 & 1484 & 1597 & 1783 & 4730 & 8179 & 3892 \\ 5685 & 5368 & 7875 & 9527 & 5235 & 3599 & 4013 & 3037 \\ 8870 & 5971 & 6474 & 9123 & 8197 & 6352 & 6427 & 4915 \\ 3381 & 3462 & 3990 & 5929 & 2438 & 3465 & 2059 & 2320 \\ 5903 & 1375 & 2245 & 9381 & 5104 & 4471 & 6319 & 6286 \\ 7275 & 4799 & 1355 & 2963 & 2684 & 2497 & 1509 & 3387 \\ 4638 & 3516 & 8850 & 6169 & 4227 & 7161 & 2471 & 9633 \\ 2953 & 2477 & 2240 & 1136 & 1745 & 1418 & 2482 & 9352 \\ 1323 & 2598 & 3270 & 2126 & 5699 & 4806 & 5428 & 8261 \\ 6672 & 3397 & 2715 & 8424 & 2132 & 7514 & 3122 & 5505 \\ 3101 & 6473 & 9497 & 9110 & 3248 & 9375 & 2459 & 3859 \\ 2383 & 9044 & 4122 & 2911 & 7737 & 5314 & 2918 & 3245 \\ 9479 & 8909 & 5374 & 2118 & 5837 & 3420 & 7277 & 2670 \\ 1652 & 4648 & 9755 & 1278 & 6236 & 6710 & 9561 & 8092 \\ 9982 & 2058 & 6265 & 8686 & 5055 & 2857 & 2461 & 7385 \end{bmatrix} \leftarrow \text{rand} \in (0,10000)$$

- **Fitness Function:** after the generation of the initial population, fitness values in the direction of the optimal solution are computed. The entry of each chromosome is transferred into the coordinate position of the sensor by using (20).

$$\begin{pmatrix} X_i \\ Y_i \end{pmatrix} = \begin{pmatrix} abs\left(\frac{\phi_{ij}}{A}\right) \\ (\phi_{ij}) \bmod(A) \end{pmatrix} \tag{20}$$

Hence, the population  $pp_1$  for the first row is converted into a sensor coordinate position by using Equation (20), the random deployment of targets, and  $pp_2$  row 1 is shown in Figures 1 and 2.

$$pp_1 \rightarrow \text{row1} \begin{pmatrix} X \\ Y \end{pmatrix} = \begin{pmatrix} 23 & 87 & 91 & 80 & 94 & 61 & 83 & 89 \\ 47 & 90 & 76 & 18 & 70 & 65 & 39 & 82 \end{pmatrix}$$

$$pp_2 \rightarrow \text{row1} \begin{pmatrix} X \\ Y \end{pmatrix} = \begin{pmatrix} 29 & 24 & 22 & 11 & 17 & 14 & 24 & 93 \\ 53 & 77 & 40 & 36 & 45 & 18 & 82 & 52 \end{pmatrix}$$

- **One Point Crossover:** exchanging the genes in the random point from the selected population matrices generates new offspring. GA uses the random value for a one-point crossover operation. Therefore, offspring1 and offspring2 are formed randomly using crossover point 4, whereas the genes are interchanged from  $pp_1$  and  $pp_2$ .

$$os1 = \begin{bmatrix} 2347 & 8790 & 9176 & 8018 & 1745 & 1418 & 2482 & 9352 \\ 3772 & 9335 & 1484 & 1597 & 5699 & 4806 & 5428 & 8261 \\ 5685 & 5368 & 7875 & 9527 & 2132 & 7514 & 3122 & 5505 \\ 8870 & 5971 & 6474 & 9123 & 3248 & 9375 & 2459 & 3859 \\ 3381 & 3462 & 3990 & 5929 & 7737 & 5314 & 2918 & 3245 \\ 5903 & 1375 & 2245 & 9381 & 5837 & 3420 & 7277 & 2670 \\ 7275 & 4799 & 1355 & 2963 & 6236 & 6710 & 9561 & 8092 \\ 4638 & 3516 & 8850 & 6169 & 5055 & 2857 & 2461 & 7385 \end{bmatrix}$$

$$os2 = \begin{bmatrix} 2953 & 2477 & 2240 & 1136 & 9470 & 6165 & 8339 & 8982 \\ 1323 & 2598 & 3270 & 2126 & 1783 & 4730 & 8179 & 3892 \\ 6672 & 3397 & 2715 & 8424 & 5235 & 3599 & 4013 & 3037 \\ 3101 & 6473 & 9497 & 9110 & 8197 & 6352 & 6427 & 4915 \\ 2383 & 9044 & 4122 & 2911 & 2438 & 3465 & 2059 & 2320 \\ 9479 & 8909 & 5374 & 2118 & 5104 & 4471 & 6319 & 6286 \\ 1652 & 4648 & 9755 & 1278 & 2684 & 2497 & 1509 & 3387 \\ 9982 & 2058 & 6265 & 8686 & 4227 & 7161 & 2471 & 9633 \end{bmatrix}$$

Offspring1 and offspring2 are obtained from the first four columns of the same parent population ( $pp_1$  and  $pp_2$ ) and the last four columns of another parent population ( $pp_2$  and  $pp_1$ ) respectively.

- **Mutation:** normally, the mutation is used after the crossover to improve the fitness of any chromosome gene by changing a randomly selected mutation point of offspring1 and offspring2. GA chooses mutation points 3 and 6 at random for offspring1 and offspring2, respectively, so that the 3rd and 6th column of offspring1 and offspring2 generates random values again.

$$os1 = \begin{bmatrix} 2347 & 8790 & 7465 & 8018 & 1745 & 1418 & 2482 & 9352 \\ 3772 & 9335 & 6694 & 1597 & 5699 & 4806 & 5428 & 8261 \\ 5685 & 5368 & 1361 & 9527 & 2132 & 7514 & 3122 & 5505 \\ 8870 & 5971 & 3626 & 9123 & 3248 & 9375 & 2459 & 3859 \\ 3381 & 3462 & 6082 & 5929 & 7737 & 5314 & 2918 & 3245 \\ 5903 & 1375 & 4097 & 9381 & 5837 & 3420 & 7277 & 2670 \\ 7275 & 4799 & 4009 & 2963 & 6236 & 6710 & 9561 & 8092 \\ 4638 & 3516 & 3414 & 6169 & 5055 & 2857 & 2461 & 7385 \end{bmatrix}$$

$$os\ 2 = \begin{bmatrix} 2953 & 2477 & 2240 & 1136 & 9470 & 8462 & 8339 & 8982 \\ 1323 & 2598 & 3270 & 2126 & 1783 & 8905 & 8179 & 3892 \\ 6672 & 3397 & 2715 & 8424 & 5235 & 3169 & 4013 & 3037 \\ 3101 & 6473 & 9497 & 9110 & 8197 & 4337 & 6427 & 4915 \\ 2383 & 9044 & 4122 & 2911 & 2438 & 5903 & 2059 & 2320 \\ 9479 & 8909 & 5374 & 2118 & 5104 & 8667 & 6319 & 6286 \\ 1652 & 4648 & 9755 & 1278 & 2684 & 9697 & 1509 & 3387 \\ 9982 & 2058 & 6265 & 8686 & 4227 & 2887 & 2471 & 9633 \end{bmatrix}$$

- Local Search: the updated offspring1 and offspring2 are used in various decomposition levels utilizing the 2D db4 lifting wavelet transform, as explained in section 4 from Equation (15) to (19), to increase the quality of potential position of deterministic sensor placements for maximum target coverage. After applying 2D db4 lifting wavelet transform some approximate and detailed component values are found negative or out of region size. To bring all the sensors into the region, a simple threshold factor (21) is applied to the jth level of child matrices and child 1 row 1 has shown in Figure 6.

$$\phi_{ij} = (|abs(\phi_{ij})| \bmod A * A) \quad (21)$$

$$ch\ 1 = \begin{bmatrix} 2236 & 2336 & 5630 & 1216 & 132 & 310 & 410 & 2647 \\ 2355 & 1255 & 6277 & 1003 & 2192 & 2253 & 3155 & 1886 \\ 4086 & 4545 & 3855 & 5329 & 7252 & 5302 & 5592 & 3637 \\ 2656 & 217 & 27 & 3171 & 190 & 1405 & 346 & 115 \\ 522 & 4696 & 2094 & 1157 & 5942 & 1410 & 1222 & 2865 \\ 316 & 2394 & 729 & 3460 & 610 & 2716 & 1187 & 1904 \\ 1510 & 3906 & 3738 & 1404 & 1326 & 1329 & 2269 & 1592 \\ 2748 & 991 & 3075 & 1008 & 3343 & 197 & 4443 & 2278 \end{bmatrix}$$

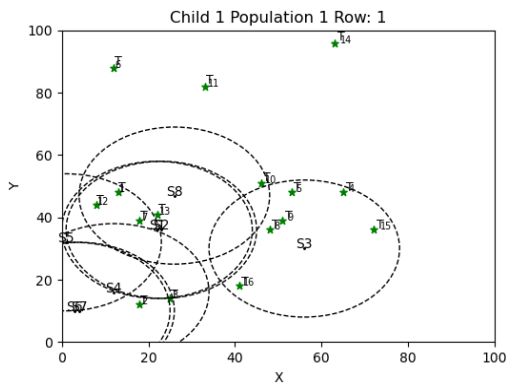
$$ch\ 2 = \begin{bmatrix} 1206 & 1444 & 3444 & 0 & 920 & 1570 & 2692 & 2041 \\ 1644 & 1137 & 1301 & 137 & 5683 & 4544 & 6617 & 1726 \\ 3256 & 456 & 1620 & 335 & 9470 & 1235 & 3947 & 867 \\ 359 & 3422 & 138 & 3944 & 3057 & 195 & 3051 & 598 \\ 709 & 742 & 7363 & 1567 & 2190 & 2687 & 257 & 956 \\ 995 & 4128 & 2802 & 302 & 2349 & 1559 & 4025 & 979 \\ 884 & 6149 & 7618 & 2620 & 175 & 2616 & 3832 & 4887 \\ 1788 & 4780 & 2487 & 5583 & 2843 & 2536 & 3999 & 383 \end{bmatrix}$$


Figure 6. Child 1 row 1 sensor deployment.

## 6. Simulation Results and Discussion

The series of simulation experiments were conducted in Python3.7 (cyclor0.10.0, decorator4.4.2, kiwisolver1.2.0, matplotlib3.2.1, networkx2.4, numpy1.18.4, pyparsing2.4.7, python-dateutil2.8.1, six1.14.0, PyWavelets1.1.1) to measure the performance of the proposed novel GA with 2-D Discrete db4 lifting wavelet transform (nGA+db4). It is

compared to existing methods such as RD and based deployment GA. The targets and sensors are deployed randomly in the 100X100, 500X500, and 1000X1000 regions. Sensor counts vary from 8 to 256, target point counts range from 16 to 512, and sensor sensing ranges range from 50 to 250.

The optimal sensor deployment problem was carried out only when the number of sensor count is less than the number of target points count, whereas ( $S(n) \leq T(m)$ ). Therefore, the simulation was conducted with different target counts as  $(\sqrt{2}, \sqrt{4}, \text{ and } \sqrt{6}) * S(n)$ , i.e.,  $T(m) = \sqrt{2} * S(n)$ ,  $T(m) = \sqrt{4} * S(n)$ , and  $T(m) = \sqrt{6} * S(n)$ . Using nGA+db4, the optimal sensor location is discovered and validated by QPS where QPS is the number of target points covered over the given region by randomly deployed connected sensors. The proposed strategy was validated using several circumstances in this experiment.

### 6.1. Varying Sensing Range of Sensors with A Fixed Target Count

In this section, the proposed algorithm was validated using different sensing ranges of the sensor as 50 to 250, sensor counts were 8 to 256 and target counts are fixed as  $T(m) = \sqrt{4} * S(n)$ . The simulation was carried out on 100X100, 500X500, and 1000X1000 regions.

In Table, 1, the QPS (%) of target coverage in the potential position of sensors was increased gradually based on two reasons:

1. When the number of sensors was increased.
2. When the sensing range of sensors was increased.

The sensors were deployed in region size 100X100 to cover a minimum of 75% and a maximum of 90% of targets in the proposed method. Table 2 shows that when the region size was increased, the target coverage ratio also increases while increasing the sensing range of sensors. Therefore, the maximum target coverage is 92%. In Table 3, the maximized sensing range of the sensor has a maximum number of target cover in given ratios. The maximum coverage was achieved here from 90% to 95%.

### 6.2. Fixed Sensing Range of Sensors with A Fixed Target Count

In this section, the proposed nGA+db4 method was validated by a fixed sensing range of the sensor is 150 and a fixed target count  $T(m) = \sqrt{6} * S(n)$ . The sensors are varied from 8 to 256 and simulation regions are 100X100, and 500X500. The quality of the potential position is to be identified to cover the maximum number of target points shown in Figures 7, and 8.

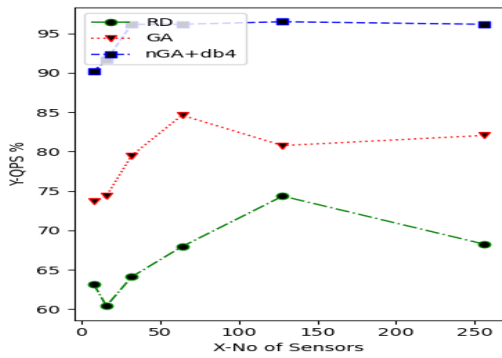


Figure 7. Number of Sensors deployed in 100X100 region vs QPS (%).

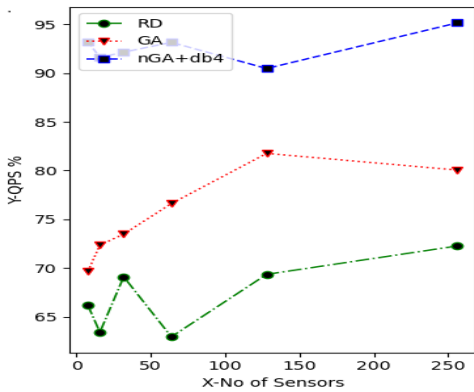


Figure 8. Number of Sensors deployed in 500X500 region vs QPS (%).

Figures 7, and 8. shows that the RD target coverage ratio is very less with a minimum of 60% and a maximum of 70%. The GA shows that a minimum of 70% and a maximum of 85% of targets were covered. The QPS of the proposed method nGA+db4 achieved above 90% with a different number of sensors counts.

### 6.3. Varying Sensing Range of Sensors with Varying Target Counts

QPS identified for a varying sensing range of sensors were 50 and 250 and a varying number of targets with scenario (Sc1)  $T(m) = \sqrt{2} * S(n)$ , and scenario (Sc2)  $T(m) = \sqrt{6} * S(n)$ . The sensor nodes were deployed in 1000X1000 monitoring environment regions and the

average QPS (%) was identified with different sensor counts.

The average QPS of sensors covered in the proposed method has gradually increased from 84%, 93% respectively for (Sc1) and (Sc2) as shown in Table 4. The maximum QPS was achieved from (Sc2) in which sensor count 256 covers 95% of target points.

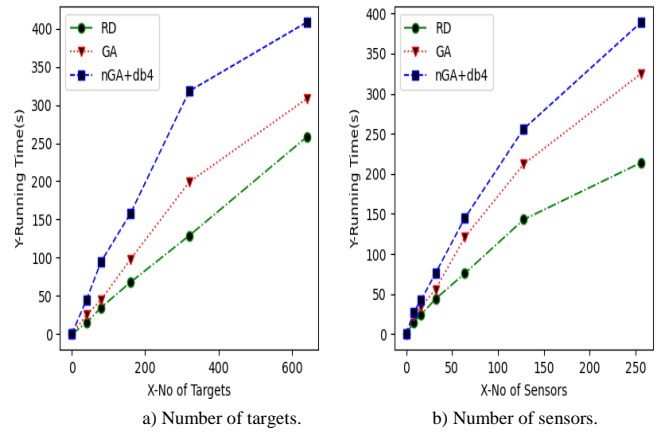


Figure 9. Running time (s).

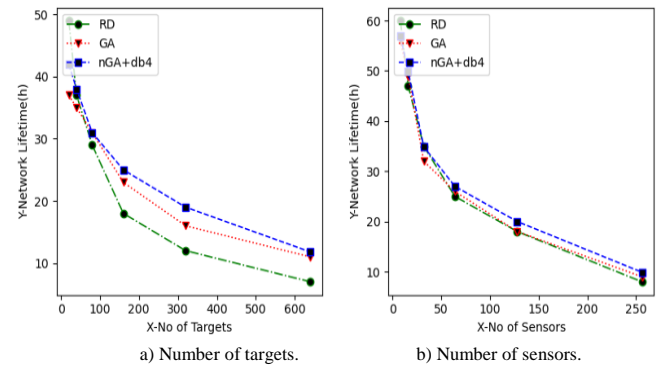


Figure 10. Network lifetime (h).

The time complexity (seconds) of the proposed algorithm is measured based on; a. number of targets and b. the number of sensor nodes in the region 1000X1000 as shown in Figure 9. The network lifetime (hours) of deployed sensor nodes was identified with the help of; a. number of targets b. the number of sensor nodes as demonstrated in Figure 10 in the region 1000X1000.

Table 1. Qps % generated for sensing range 50 and  $T(m) = \sqrt{4} * S(n)$ .

S(n)	100x100						500x500					
	RD		GA		nGA+db4		RD		GA		nGA+db4	
	Min QPS	Max QPS										
8	31.25	43.75	37.50	56.25	62.50	75.00	25.00	37.50	37.50	68.75	56.25	81.25
16	34.37	46.87	43.75	68.75	65.62	84.37	28.12	43.75	46.87	71.87	59.37	84.37
32	32.81	51.56	42.18	67.18	60.93	85.93	40.62	59.37	45.31	73.43	60.93	89.06
64	43.75	56.25	53.90	68.75	59.37	87.50	56.25	68.75	57.81	71.87	67.18	88.28
128	46.87	60.15	53.12	76.56	64.84	87.10	52.73	68.35	56.25	78.12	66.79	90.62
256	50.00	60.93	59.96	79.10	64.06	89.06	53.90	71.48	66.99	80.46	70.11	95.70

Table 2. QPS % produced for sensing range 150 and  $T(m) = \sqrt{4} * S(n)$ .

S(n)	500x500						1000x1000					
	RD		GA		nGA+db4		RD		GA		nGA+db4	
	Min QPS	Max QPS	Min QPS	Max QPS	Min QPS	Max QPS	Min QPS	Max QPS	Min QPS	Max QPS	Min QPS	Max QPS
8	37.5	56.25	43.75	68.75	50.00	81.25	37.50	62.50	43.75	75.00	56.25	81.25
16	43.75	65.62	46.87	75.00	53.12	81.25	40.62	65.62	46.87	78.12	56.25	84.37
32	43.75	75.00	51.56	78.12	56.25	82.81	45.31	68.75	48.43	78.12	57.81	84.37
64	40.62	71.87	53.90	78.12	54.68	86.71	46.09	74.21	51.56	80.46	54.68	86.71
128	47.65	69.53	54.29	78.90	54.29	86.32	46.09	72.65	51.56	78.51	55.85	84.76
256	50.00	73.82	53.12	79.10	58.59	91.79	48.82	71.48	51.95	81.05	58.59	91.60

Table 3. QPS % generated for sensing range 250 and  $T(m) = \sqrt{4} * S(n)$ .

S(n)	100x100						1000x1000					
	RD		GA		nGA+db4		RD		GA		nGA+db4	
	Min QPS	Max QPS	Min QPS	Max QPS	Min QPS	Max QPS	Min QPS	Max QPS	Min QPS	Max QPS	Min QPS	Max QPS
8	43.75	62.50	50.00	75.00	56.25	87.50	50.00	75.00	56.25	81.25	62.50	87.50
16	43.75	68.75	56.25	78.12	62.50	90.62	53.12	78.12	59.37	84.37	62.50	87.50
32	46.87	68.75	54.68	76.56	64.06	89.06	56.25	76.56	62.50	82.81	64.06	90.62
64	48.43	73.43	56.25	85.15	67.18	90.62	54.68	79.68	61.71	80.46	64.06	92.18
128	50.00	71.87	60.54	87.89	65.62	89.45	54.29	77.73	64.45	82.81	67.18	92.18
256	50.58	70.11	67.57	86.71	65.03	90.82	53.51	78.51	67.96	83.20	69.53	94.92

Table 4. Average QPS % of Sensing Range 50 and 250 and Sc1 and Sc2.

S(n)	Sensing Range 50						Sensing Range 250					
	RD		GA		nGA+db4		RD		GA		nGA+db4	
	T(m)		T(m)		T(m)		T(m)		T(m)		T(m)	
	Sc1	Sc2	Sc1	Sc2	Sc1	Sc2	Sc1	Sc2	Sc1	Sc2	Sc1	Sc2
8	62.34	64.56	73.45	77.56	82.56	84.18	69.56	73.45	77.67	84.78	90.25	93.45
16	63.45	65.45	74.45	77.56	83.56	89.78	70.15	75.25	79.56	86.35	91.25	93.56
32	67.56	69.67	76.25	79.45	83.56	90.15	72.15	74.15	80.45	88.81	92.25	92.45
64	67.56	70.25	76.25	80.75	84.70	89.75	73.50	75.50	84.45	90.25	93.25	94.45
128	69.45	72.45	79.56	82.25	85.75	90.25	74.57	77.56	83.57	90.25	92.45	93.25
256	70.75	74.45	80.45	83.35	87.87	90.15	74.15	76.45	83.45	89.75	91.45	94.15

## 7. Conclusions

The problem of sensor node deployment and node connectivity describes a novel technique called nGA-2DD db4 lifting wavelet transform to identify the optimal sensor node location to monitor the maximum number of targets with connected nodes. To proceed, the nGA-based population matrix gives sensor coordinates for evaluating the fitness function of sensor placements. The solution is further applied to local enhancement based on 2D discrete db4 lifting wavelet transform to adjust the sensor position to an optimal state. The result of the proposed algorithm has shown the ability to cover the maximum number of targets and enabled node connectivity by a series of simulation results with a different setup. The simulation results are demonstrated with a set of scenarios that demonstrate the efficiency and superiority of proposed methods with maximum target coverage ratio with the least number of sensor nodes and longer network lifetime. In the future, more experimental setup will be necessary to test the performance of data gathering from sensor nodes in real-world sensor networks.

## References

[1] Abdelkhalek O., Krichen S., and Guitouni A, “A Genetic Algorithm-Based Decision Support

System for the Multi-Objective Node Placement Problem in Next Wireless Generation Network,” *Applied Soft Computing*, vol. 33, pp. 278-291, 2015.

[2] Abo-Zahhad M., Sabor N., Sasaki S., and Ahmed S., “A Centralized Immune-Voronoi Deployment Algorithm for Coverage Maximization and Energy Conservation in Mobile Wireless Sensor Networks,” *Information Fusion*, vol. 30, pp. 36-51, 2016.

[3] Ashouri M., Zali Z., Mousavi S., and Hashemi M., “New Optimal Solution to Disjoint Set k-Coverage for Lifetime Extension in Wireless Sensor Networks,” *IET Wireless Sensor Systems*, vol. 2, no. 1, pp. 31-39, 2012.

[4] Bamerni S. and Kh.Al-Sulaifanie A., “An Efficient Non-Separable Architecture for Haar Wavelet Transform with Lifting Structure,” *Microprocessors and Microsystems*, vol. 71, no. 1, pp. 1-7, 2019.

[5] Bouzid S., Seresstou Y., Raouf K., Omri M., Mbarki M., and Dridi C., “MOONGA: Multi-Objective Optimization of Wireless Network Approach Based on Genetic Algorithm,” *IEEE Access*, vol. 8, pp. 105793-105814, 2020.

[6] Chen C., Mukhopadhyay S., Chuang C., Lin T., Liao M., Wang Y., and Jiang J., “A Hybrid Memetic Framework for Coverage Optimization in Wireless Sensor Networks,” *IEEE Transactions*

- on Cybernetics, vol. 45, no. 10, pp. 2309-2321, 2015.
- [7] Elhoseny M., Tharwat A., Yuan X., and Hassanien A., "Optimizing K-Coverage of Mobile WSNs," *Expert Systems with Applications*, vol. 92, no. 4, pp. 142-153, 2018.
- [8] Fan T. and Chen J., "A New Nonuniform Random Deployment Method to Minimize Cost for Large-Scale Wireless Sensor Networks," *IEEE Access*, vol. 8, pp. 198532-198547, 2020.
- [9] Ganesan T. and Rajarajeswari P., "A Novel Genetic Algorithm with 2D CDF 9/7 Lifting Discrete Wavelet Transform for Total Target Coverage in WSNs Deployment," *International Journal of Communication Networks and Distributed Systems*, vol. 26, no. 4, pp. 464-483, 2021.
- [10] Ganesan T. and RajaRajeswari P., "Hybrid Genetic Algorithm with Haar Wavelet for Maximum Target Coverage Node Deployment in Wireless Sensor Networks," *Journal of Cases on Information Technology*, vol. 23, no. 3, pp. 78-95 2021.
- [11] Ganesan T., Rajarajeswari P., Nayak S., and Bhatia A., "A Novel Genetic Algorithm with CDF5/3 Filter-based Lifting Scheme for Optimal Sensor Placement," *International Journal of Innovative Computing and Applications*, vol. 12, no. 2-3, pp. 67-76, 2021.
- [12] Gupta S., Kuila P., and Jana P., "Genetic Algorithm Approach for K-Coverage and m Connected Node Placement in Target-based Wireless Sensor Networks," *Computers and Electrical Engineering*, vol. 56, pp. 544-556, 2015.
- [13] Hanh N., Binh H., Hoai N., and Palamiswami MS., "An Efficient Genetic Algorithm for Maximizing Area Coverage in Wireless Sensor Networks," *Information Sciences*, vol. 488, no. 1, pp. 58-75, 2019.
- [14] Harizan S. and Kuila P., "A Novel NSGA-II for Coverage and Connectivity Aware Sensor Node Scheduling in Industrial Wireless Sensor Networks," *Digital Signal Processing*, vol. 105, pp. 102753, 2020.
- [15] Hasan M. and Wahid K., "Low-Cost Architecture of Modified Daubechies Lifting Wavelets using Integer Polynomial Mapping," *IEEE Transactions on Circuits and Systems II*, vol. 64, no. 5, pp. 585-589, 2016.
- [16] Hasan R., Abdulwahid H., and Abdalzahra A., "Using Ideal Time Horizon for Energy Cost Determination," *Iraqi Journal for Computer Science and Mathematics*, vol. 2, no. 1, pp. 9-13, 2021.
- [17] Hasan R., Shahab S., and Ahmed M., "Correlation with the Fundamental PSO and PSO Modifications to be Hybrid Swarm Optimization," *Iraqi Journal for Computer Science and Mathematics*, vol. 2, no. 2, pp. 25-32, 2021.
- [18] Hossam A., Salem T., Abdlhady A., and Abd el-kader S., "MCA-MAC: Modified Cooperative Access MAC Protocol in Wireless Sensor Networks," *The International Arab Journal of Information Technology*, vol. 18, no. 3, pp. 326-335, 2021.
- [19] Hu X., Zhang J., Yu Y., Chung H., Li H., Shi Y., and Luo X., "Hybrid Genetic algorithm Using Forward Encoding Scheme for Lifetime Maximization of Wireless Sensor Networks," *IEEE Transaction on Evolutionary Computation*, vol. 14, no. 5, pp. 766-780, 2010.
- [20] Karimi-Bidhendi S., Guo J., and Jafarkhani H., "Energy-Efficient Node Deployment in Heterogeneous Two-Tier Wireless Sensor Networks with Limited Communication Range," *IEEE Transactions on Wireless Communications*, vol. 20, no. 1, pp. 40-55, 2021.
- [21] Katii A., "Target Coverage in Random Wireless Sensor Networks Using Cover Sets," *Journal of King Saud University-Computer and Information Sciences*, vol. 34, no. 3, pp. 734-746, 2019.
- [22] Kim J. and Yoo Y., "Sensor Node Activation Using Bat Algorithm for Connected Target Coverage in WSNs," *Sensors*, vol. 20, no. 13, pp. 3733, 2020.
- [23] Liao C. and Ting C., "A Novel Integer-Coded Memetic Algorithm for the Set k-Cover Problem in Wireless Sensor Networks," *IEEE Transactions on Cybernetics*, vol. 48, no. 8, pp. 2245-2258, 2017.
- [24] Liu Y., chin K., Yang C., and He T., "Node's Deployment for Coverage in Rechargeable Wireless Sensor Networks," *IEEE Transaction on Vehicular Technology*, vol. 68, no. 6, pp. 6064-6073, 2019.
- [25] Mini S., Udgata S., and Sabat S., "Sensor Deployment and Scheduling for Target Coverage Problem in Wireless Sensor Networks," *IEEE Sensors Journal*, vol. 14, no. 3, pp. 636-644, 2014.
- [26] Moh'd Alia O. and Al-Ajourri A., "Maximizing Wireless Sensor Network Coverage with Minimum Cost Using Harmony Search Algorithm," *IEEE Sensors Journal*, vol. 17, no. 3, pp. 882-896, 2017.
- [27] Nguyen P., Hanh N., Khuong N., Khuong N., Binh H., and Ji Y., "Node Placement for Connected Target Coverage in Wireless Sensor Networks With Dynamic Sinks," *Pervasive and Mobile Computing*, vol. 59, no. 2, pp. 1-21, 2019.
- [28] Njoya A., Thron C., Barry J., Abdou W., Tonye E., Konje N., and Dipanda A., "Efficient Scalable Sensor Node Placement Algorithm for Fixed Target Coverage Applications of Wireless Sensor

- Networks,” *IET Wireless Sensor Systems*, vol. 7 no. 2, pp. 44-54, 2017.
- [29] Pal P., Sharma R., Tripathi S., Kumar C., and Ramesh D., “Genetic Algorithm Optimized Node Deployment in IEEE 802.15.4 Potato and Wheat Crop Monitoring Infrastructure,” *Scientific Reports*, vol. 11, no. 1, pp. 8231, 2021.
- [30] Sharma V., Srivastava D., and Mathur P., “A Daubechies DWT Based Image Steganography Using Smoothing Operation,” *The International Arab Journal of Information Technology*, vol. 17, no. 2, pp. 154-161, 2020.
- [31] Tian X., Wu L., Tan Y., and Tian J., “Efficient Multi-Input/Multi-Output VLSI Architecture for Two-Dimensional Lifting-Based Discrete Wavelet Transform,” *IEEE Transactions on Computers*, vol. 60, no. 8, pp. 1207-1211, 2011.
- [32] Vijayaraju P., Sripathy B., Arivudainambi D., and Balaji S., “Hybrid Memetic Algorithm with Two-Dimensional Discrete Haar Wavelet Transform for Optimal Sensor Placement,” *IEEE Sensors Journal*, vol. 17, no. 7, pp. 2267-2278, 2017.
- [33] Vilela J., Kashino Z., Ly R., Nejat G., and Benhabib B., “A Dynamic Approach to Sensor Network Deployment for Mobile-Target Detection in Unstructured, Expanding Search Areas,” *IEEE Sensors Journal*, vol. 16, No. 11, pp. 4405-4417, 2016.
- [34] Yoon Y. and Kim Y., “An Efficient Genetic Algorithm for Maximum Coverage Deployment in Wireless Sensor Networks,” *IEEE Transaction Cybernetics*, vol. 43, no. 5, pp.1473-1483, 2013.
- [35] Zhang Y. and Liu M., “Node Placement Optimization of Wireless Sensor Networks Using Multi-Objective Adaptive Degressive Ary Number Encoded Genetic Algorithm,” *Algorithms*, vol. 13, no. 8, pp. 189, 2021.
- [36] Zhang Y., Gong Y., Gu T., Li Y., and Zhang J., “Flexible Genetic Algorithm: A Simple and Generic Approach to Node Placement Problems,” *Applied Soft Computing*, vol. 52, pp. 1-14, 2016.



**Ganesan Thangavel** is currently working as an Assistant Professor in the Department of CSE at Koneru Lakshmaiah Education Foundation (KLEF), India, where he is currently pursuing his Ph.D. He has completed his BTech and MTech from Anna University, India. He published several research papers in reputed journals. His research interest includes wireless sensor network, genetic algorithm, and machine learning.



**Pothuraju Rajarajeswari** received her Doctorate in Computer Science and Engineering and Ph.D. in CSE in 2012 from Acharya Nagarjuna University. Currently, she is working as a Professor in the Department of CSE in Koneru Lakshmaiah Education Foundation (KLEF). She has professional memberships in FIETE, MISTE, MIACSIT in the International Association of Computer Science and Information Technology, and MIAENG in the International Association of Engineers. She has 19 years of experience in teaching computer subjects for BTech, MCA, and MTech Postgraduate students. Her research interests are bioinformatics, data mining, artificial intelligence, and data science.